Received: 28 February 2019 | Revised: 19 April 2019 | Accepted: 22 April 2019

DOI: 10.1002/col.22384

RESEARCH ARTICLE

WILEY

Chromatic adaptation transform by spectral reconstruction

Scott A. Burns

Industrial & Enterprise Systems Engineering, Grainger College of Engineering, University of Illinois at Urbana-Champaign, Urbana, Illinois

Correspondence
Scott A. Burns, Industrial & Enterprise Systems Engineering, Grainger College of Engineering, University of Illinois at Urbana-Champaign, Urbana, IL.
Email: scottb@illinois.edu

Abstract

A color appearance model (CAM) is an advanced colorimetric tool used to predict color appearance under a wide variety of viewing conditions. A chromatic adaptation transform (CAT) is an integral part of a CAM. Its role is to predict "corresponding colors," that is, a pair of colors that have the same color appearance when viewed under different illuminants, after partial or full adaptation to each illuminant. Modern CATs can sometimes generate colors with negative tristimulus values. For some imaging applications, it is important to maintain positive tristimulus values when applying a CAT. This article proposes a new CAT that does not operate on the standard von Kries model of adaptation. Instead, it uses a spectral reconstruction technique as an intermediate stage in the process, while still requiring only tristimulus values as inputs. It is demonstrated that the proposed CAT will not generate colors outside the spectral locus or colors with negative tristimulus values. The proposed CAT does not use established empirical corresponding-colors data sets to optimize performance, as most modern CATs do, yet it performs as well as or better than the most recent CATs when tested against the data sets of corresponding colors.

KEYWORDS

chromatic adaptation, color appearance models, color constancy, reflectance, spectral reconstruction

1 | INTRODUCTION

A color appearance model (CAM) is an advanced colorimetric tool used to predict color appearance under a wide variety of viewing conditions.[1,2] A chromatic adaptation transform (CAT) is an integral part of a CAM. Its role is to predict "corresponding colors," that is, a pair of colors that have the same color appearance when one is viewed under one illuminant and the other is viewed under a different illuminant.[3] It is assumed that the viewer is adapted, or partially adapted, to the illuminants before assessing color appearance.

Most CATs are based on the von Kries coefficients law.[4] The tristimulus values of a source sample are transformed to cone-response space (or something similar, such as a "sharpened" version), and then the cone response magnitudes are scaled by the ratios of destination-to-source illuminant white point cone-response magnitudes. A final transformation back to tristimulus value space yields the predicted destination color. The transformation is usually modified to account for partial adaptation using a parameter D that ranges between 0 and 1.

Note that the terms "source" and "destination" used here differ from the alternate terminology of "test" and "reference" often found in the literature. If the latter terms are preferred, simply replace "source" with "test" and "destination" with "reference" in the development that follows.

Several experimental data sets of corresponding colors have been compiled to aid in the development of modern CATs. The standard data sets used in the development of recent CATs are known as CSAJ, Helson, Lam & Rigg, LUTCHI, Kuo & Luo, Breneman, Braun & Fairchild, and McCann.[5] The numerical data are no longer available at the

URL provided in Reference 5, but they can be obtained through a web archive site.[6]

Some von-Kries-type CATs are theoretical, that is, they do not rely on the experimental corresponding-colors data sets for their development. Instead, they are derived from the results of well-established physiological studies, such as spectral cone-sensitivity functions or cone signal compression phenomena. In contrast, many recent CATs are derived with the aid of the empirical corresponding-colors data sets. The transformation that converts tristimulus values into cone responses is modified through an optimization to yield a CAT that produces corresponding colors that match the empirical data more closely, sometimes including constraints in the optimization formulation to enforce additional desirable behaviors.[7-13] Examples of these empirically "trained" CATs include Bradford (BFD), CMCCAT97, CMCCAT2000, CAT02, and most recently CAT16.[13-15]

One characteristic of linear von-Kries-type CATs is that they can sometimes produce tristimulus values with negative components. While negative tristimulus values are useful for describing "supersaturated" colors,[16] negative values can be problematic in some imaging applications.[10] To address instances of when negative destination tristimulus values are undesirable, this article presents a proposed CAT that (a) will not generate destination colors that fall outside the spectral locus, including colors with negative tristimulus values, (b) performs as well as or better than all existing modern CATs when tested against the experimental corresponding-colors data sets, and (c) does not use the experimental data sets to train or fine-tune the method.

In the sections that follow, examples of modern CATs yielding negative destination tristimulus values are presented. Then the proposed CAT that makes use of a spectral reconstruction technique is outlined. Next, the mathematical optimization supporting the spectral reconstruction is presented and specifics of its numerical implementation follow that. The next two sections are concerned with symmetry and robustness of the proposed CAT. Finally, a treatment for partial adaptation within the framework of the new CAT is proposed as a direction for future research.

2 | EXAMPLES OF CATS PRODUCING NEGATIVE TRISTIMULUS VALUES

This section demonstrates how modern CATs can produce destination colors with negative tristimulus values. Three CATs are examined: two modern CATs that have been optimized to match better the empirical corresponding-colors data sets, CAT02 and CAT16, and one CAT that is not "trained" in this way, known as HPE.[17] This third CAT is a direct application of the von Kries coefficient rule using a transformation from tristimulus space to cone response space derived from Estévez's original estimates of theoretical cone sensitivity functions.[18] Full adaptation ($D = 1$) is assumed in all demonstrations presented in this section.

The source colors used in the demonstrations are drawn from the set of "object colors." If we restrict our attention to objects having reflectance properties in the range 0–1 over all visible wavelengths, then the stimuli produced by a given illuminant acting on all possible reflectances of this type project into a three-dimensional color space region called the "object color solid," the outer surface of which comprises the "optimum colors."[19]

Figure 1 shows HPE, CAT02, and CAT16 applied to a $Y = 0.3$ slice of the object color solid, using a source illuminant that is halfway between equal energy and the spectral locus (white point XYZ = [1.5, 1, 0.5] and [x, y] = [0.5, 0.333], shown in Figure 2).

Figure 1 demonstrates that a substantial portion of the object colors is projected outside of the spectral locus (red

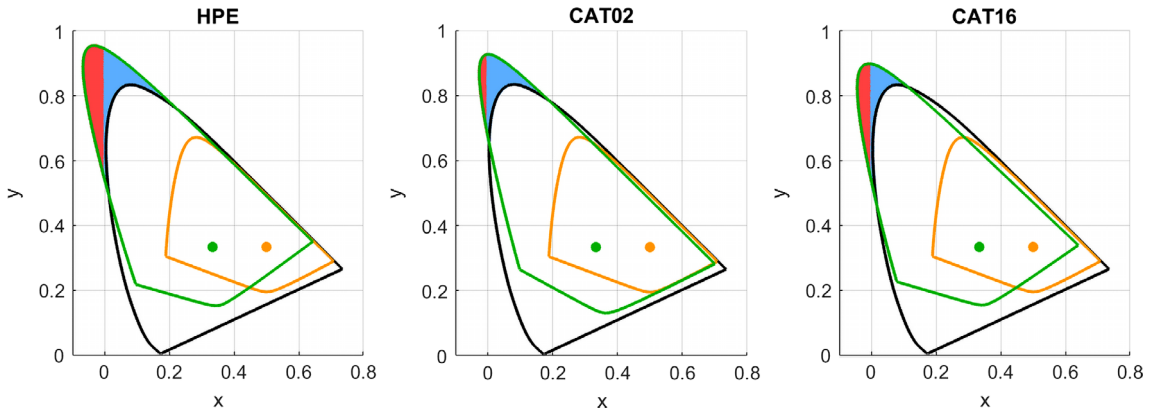

FIGURE 1 Object color solid slice for $Y = 0.3$ (orange curve) using source illuminant shown in Figure 2 (orange dot) and the transformed region (green curve) after application of HPE, CAT02, and CAT16, using equal energy as the destination illuminant (green dot). The red region has negative tristimulus values, and the red and blue regions fall outside the spectral locus (black curve)

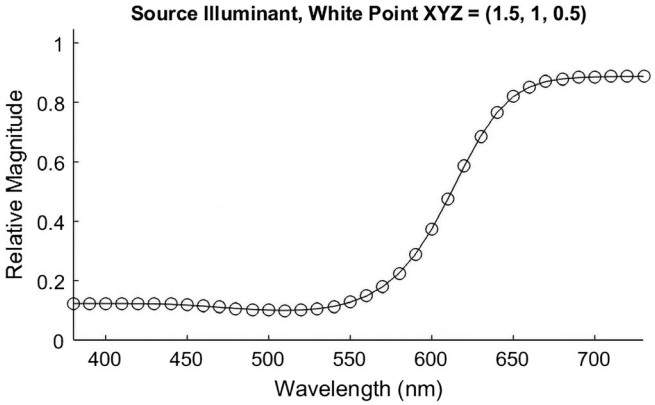

FIGURE 2 Source illuminant for the results shown in Figure 1

and blue regions) and the red region has negative destination tristimulus values. Numerical details of one instance of this behavior can be found in the online supplementary documentation.[20] The following sections present a proposed CAT that will not produce destination colors outside the spectral locus or yield negative tristimulus values.

3 | NOTATION

The symbols used in the following development are summarized in Table 1.

4 | CAT BY SPECTRAL RECONSTRUCTION

Modern CATs ignore the spectral makeup of illuminants and source/destination colors and operate only on tristimulus values. Changes in color sensations by adaptation, ostensibly due to changes in cone sensitivities, are modeled by the von Kries coefficients law. In contrast, the proposed CAT constructs spectral distributions from the tristimulus values of the source color and both illuminant white points and simply computes the effect that changing the illuminant has on tristimulus values using standard color-matching function (CMF) calculations. While this approach appears to ignore the phenomenon of adaptation, focusing instead on techniques more closely related to color constancy, the corresponding-color pairs it generates match the empirical corresponding-colors data sets as well as or better than existing CATs. It should be noted that although the proposed method uses a spectral reconstruction as an intermediate stage of the process, its inputs are the same as those for traditional CATs, namely, tristimulus values of source colors and illuminant white points.

The proposed CAT algorithm operates as follows: Given a source color, XYZ_S, which is referenced to a source illuminant with white point XYZ_S^{wp}, we seek a prediction of a corresponding color, XYZ_{Dp}, referenced to a destination

TABLE 1 Explanation of symbols

Symbol	Definition
n	Number of wavelength bands used to discretize spectral-based entities (in this presentation, all computations use $n = 36$, representing 10 nm bands spanning the range 380-730 nm).
$\bar{x},\bar{y},\bar{z}$	Three $n \times 1$ vectors of color-matching functions (the CIE 1931 standard observer is used in computations in this presentation).
A	$n \times 3$ matrix of CMFs, by columns: $A = [\bar{x},\bar{y},\bar{z}]$.
W	$n \times 1$ illuminant vector, assumed to be non-negative and scaled (normalized) so that the scalar product $\bar{y}' \cdot W = 1$ (prime denotes transpose. Subscripts denote different illuminants, eg, W_S and W_D).
$\overline{W}$	$n \times n$ diagonal matrix, $\overline{W}$ = diag(W), which places W on the main diagonal and zeros elsewhere.
ρ	$n \times 1$ reflectance vector, typically with values in the range 0-1.
XYZ	3×1 vector of tristimulus values, X, Y, and Z, computed as $XYZ = A'\ \overline{W}\rho$ (note the reflective/transmissive case is used here, as opposed to the emissive case, so all tristimulus values are referenced to some illuminant, W, and a perfect reflector will yield $Y = 1$. A subscript indicates to which illuminant it is referenced, eg, XYZ_S or XYZ_D. A second subscript of "p" indicates it is a predicted quantity generated by a CAT, eg, XYZ_{Dp}).
XYZ^{wp}	3×1 vector of illuminant white point tristimulus values, $XYZ^{wp} = A'\ W$ (because of the assumed scaling of W, the Y value will always equal 1. A subscript can be added to specify the illuminant, eg, XYZ_S^{wp} or XYZ_D^{wp}).
A_W	$n \times 3$ matrix of illuminant W-referenced color-matching functions, $A_W = \overline{W}\,A$ (W-referenced tristimulus values are computed directly from reflectance as $XYZ_W = A_W'\ \rho$. The subscript is used to differentiate between various illuminants, eg, A_S and A_D).
C	$n \times n$ matrix of finite-differencing constants (see Equation 5).
A_{SD}	$n \times 3$ matrix of dual-referenced (by both source and destination illuminants) color-matching functions, $A_{SD} = \overline{W_S}\,\overline{W_D}\,A$.
D	Degree of adaptation parameter, ranging from 0 (fully unadapted) to 1 (fully adapted).

Abbreviations: CAT, chromatic adaptation transform; CMFs, color-matching functions.

TABLE 2 Mean ΔE^*_{94} color difference for HPE, CAT02, CAT16, and the proposed method

Data set	HPE	CAT02	CAT16	Proposed method
CSAJ	4.71	3.66	3.95	3.72
Helson	4.52	3.45	4.00	4.10
Lam & Rigg	4.31	2.97	3.45	3.22
LUTCHI	4.03	3.55	3.43	4.01
Kuo & Luo	4.29	3.30	3.41	2.85
Breneman	6.61	5.70	5.66	5.48
Braun & Fairchild	4.54	4.00	4.24	4.07
McCann	10.82	11.52	10.80	9.78
Mean (all data sets)	**5.54**	**4.87**	**4.91**	**4.74**
Mean (no McCann)	**4.77**	**3.91**	**4.06**	**4.01**

illuminant with white point XYZ_D^{wp} (at this point, we are assuming full adaptation).

1. Construct two normalized spectral distributions, W_S and W_D, which when treated as illuminants, have white points XYZ_S^{wp} and XYZ_D^{wp}, respectively (see Section 6 on how to generate this spectral reconstruction from the illuminant white point tristimulus values). Use these two distributions to form W_S- and W_D-referenced CMFs, $A_S = \overline{W_S}\, A$ and $A_D = \overline{W_D}\, A$.
2. Construct a reflectance curve, ρ, that satisfies $XYZ_S = A_S{}' \rho$ (see Section 6 on how to perform this reflectance reconstruction).
3. Compute $XYZ_D = A_D{}' \rho$.
4. Adjust XYZ_D so that it preserves its chromaticity coordinates, (x, y), while having a Y value that matches the Y value of XYZ_S. Call this XYZ_{Dp}.
5. XYZ_{Dp} is the predicted corresponding color associated with XYZ_S for the two illuminant white points XYZ_S^{wp} and XYZ_D^{wp}.

The fourth step above is justified by the observation that in corresponding-colors experiments, the goal of the observer is to find source and destination colors that appear identical when viewed under a state of adaptation to the respective illuminants. The experiments are designed to produce corresponding colors with similar luminances, so that luminance-dependent changes in colorfulness and contrast are not triggered (known as Hunt and Stevens effects). Indeed, 14 of the 26 standard corresponding-colors data sets (the 3 LUTCHI sets, 2 Kuo & Luo sets, and 9 Breneman sets) have corresponding color pairs with identical Y values. The mean difference of all Y values in the corresponding-colors data (excluding McCann) is 0.33 (on a 0-to-100 scale) and the SD of the differences is 1.1. Steps 1 to 3 of the algorithm above do not preserve Y values as the corresponding-colors experiments do, so it is reasonable to add step 4 to mimic this preservation.

Before examining the specifics of how to compute the spectral reconstructions above, a demonstration of the effectiveness of the proposed CAT is presented in Table 2, which compares the ΔE^*_{94} color differences between the experimental data set destination colors, XYZ_D, and the CAT-predicted destination colors, XYZ_{Dp}, for four methods: HPE, CAT02, CAT16, and the proposed CAT. In all cases, full adaptation ($D = 1$) is used. See the online supplementary documentation for more information regarding these calculations.[21]

The mean values in the last two rows of Table 2 are weighted means, that is, they represent the mean of all samples in all data sets, not the mean of the data set means. The proposed method performs favorably when all data sets are considered. Both CAT02 and CAT16 were optimized for all data sets except the McCann data set. The proposed method has a mean value that falls between the mean values of CAT02 and CAT16 when the McCann data are excluded. It should be noted that the proposed method, like the HPE method, is not optimized at all to fit the experimental corresponding-colors data sets.

One possible explanation for why the spectral reconstruction method performs so well is the observation that the type of reconstructed reflectance curve used in this study seems to match reflectance curves of object colors found in nature surprisingly well, in particular, the reflectances of common paints and pigments.[22] Figure 3 shows the spectrophotometrically measured reflectance curves of six Liquitex paints and the corresponding reflectance reconstructions generated from the tristimulus values of the paints.

Although there are considerable discrepancies in the upper and lower extremes of the visible spectrum, these deviations are largely inconsequential, as human sensitivity to these wavelengths is very low. Consequently, calculation of quantities like tristimulus values is relatively insensitive to variations in stimuli at these extreme wavelengths.

5 | SPECTRAL RECONSTRUCTION COMPUTATION

Spectral reconstruction is the process of generating a distribution (eg, reflectance, power, etc) over a wavelength (or frequency) domain, given only a three-dimensional representation of the color, such as tristimulus values referenced to some illuminant. There are many ways to generate reconstructed spectral distributions from target tristimulus values.[23-41] The solution is not unique; there is an entire

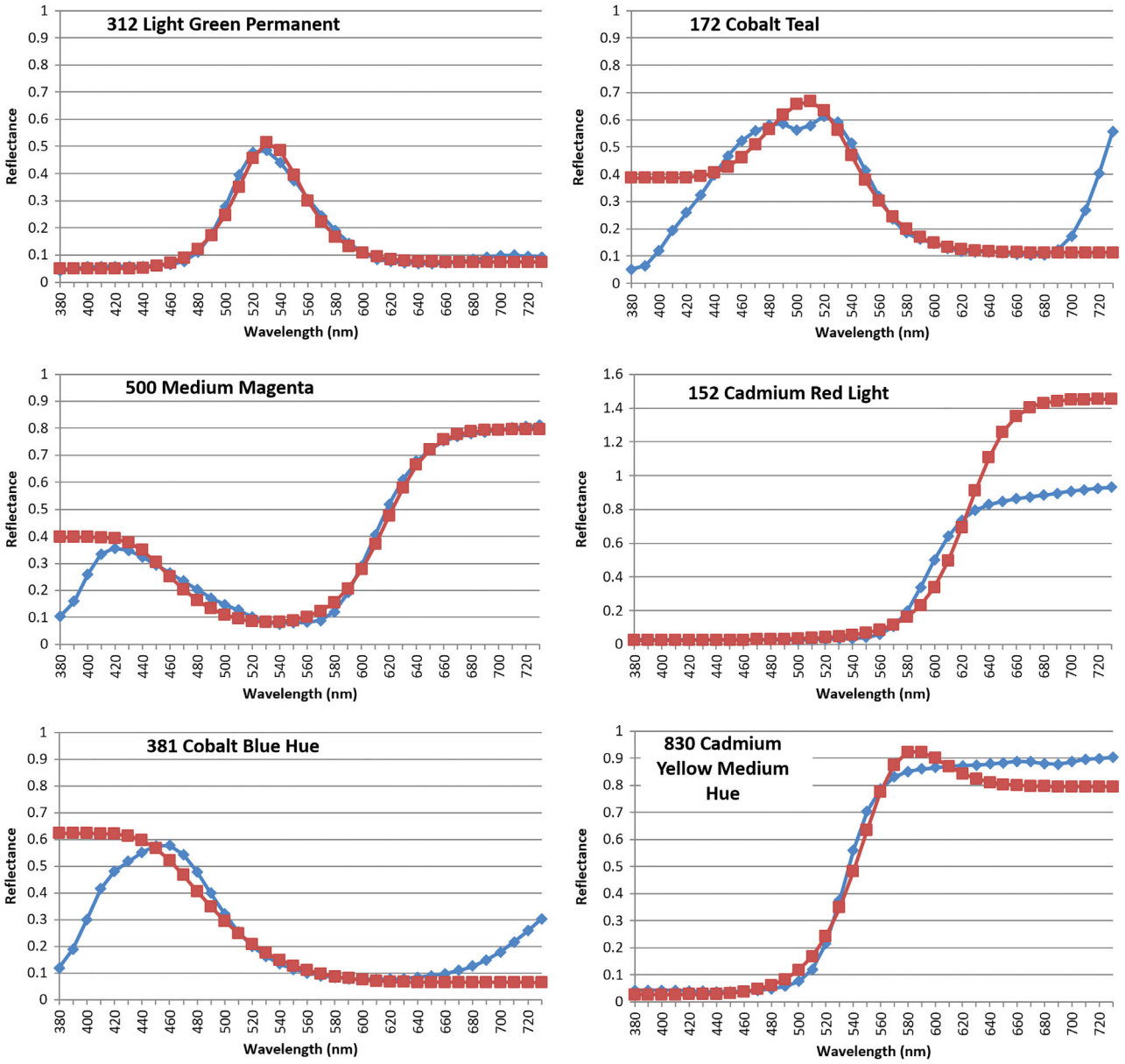

FIGURE 3 Spectrophotometrically measured reflectance curves of six Liquitex paints (blue curves) and the corresponding reflectance reconstructions generated from the tristimulus values of the paints (red curves)

"metameric suite" of spectral distributions that share common tristimulus values. The outcome of each reconstruction algorithm differs according to the assumptions and restrictions imposed on the reconstruction. Some previous work has appeared on spectral adaptation, but the goal of that work differs from that of this article.[42,43]

One way to perform the reconstruction is to identify the unique member of the metameric suite of reflectance curves, ρ, with minimum slope squared, integrated over the range of visible wavelengths, that is,

$$\min_{\rho} \int_{\text{visible } \lambda} (d\rho/d\lambda)^2 \, d\lambda, \tag{1}$$

subject to the constraint that ρ must yield the target tristimulus values. Equation (1) was originally proposed and investigated by van Trigt.[23,24] Unfortunately, this form of the optimization can sometimes lead to curves that have regions of negative reflectance. To avoid this, the present author has modified the optimization to operate in the space of $z = \ln \rho$, so the new objective function becomes

$$\min_{z} \int_{\text{visible } \lambda} (dz/d\lambda)^2 \, d\lambda. \tag{2}$$

This keeps $\rho = e^z$ strictly positive. The continuous optimization above can be discretized to make it suitable for numerical solution:

$$\min_{z} \sum_{i=1}^{n-1} (z_{i+1} - z_i)^2 \quad \text{s.t.} \quad A_S{}' e^z = XYZ_S. \tag{3}$$

Note that the constraint uses a source illuminant-referenced set of CMFs, A_S, which when transposed and multiplied by the $n \times 1$ reflectance vector, e^z, equals the target XYZ_S. Equation (3) can also be expressed fully in matrix form:

$$\min_{z} \frac{1}{2} z'Cz \quad \text{s.t.} \quad A_S{}' e^z = XYZ_S, \tag{4}$$

where C is an $n \times n$ tridiagonal matrix of finite-differencing constants,

$$C = \begin{bmatrix} 2 & -2 & & & & & \\ -2 & 4 & -2 & & & & \\ & -2 & 4 & -2 & & & \\ & & \ddots & \ddots & \ddots & & \\ & & & -2 & 4 & -2 & \\ & & & & -2 & 2 & \end{bmatrix}. \tag{5}$$

This constrained nonlinear program (NLP) is easily solved by optimization software packages. However, the computational overhead of general-purpose optimization code is unnecessary when solving an NLP with a simple structure such as this one has. A far more computationally efficient approach is to apply the method of Lagrange multipliers to this equality constrained NLP. The Lagrangian function is

$$L(z,\lambda) = \frac{1}{2} z'Cz + \lambda'(A_S{}' e^z - XYZ_S), \tag{6}$$

where λ is a 3×1 vector of Lagrange multipliers. Setting partial derivatives of the Lagrangian to zero,

$$\begin{aligned} \partial L/\partial z &= Cz + \mathrm{diag}(e^z)A_S\lambda = 0 \\ \partial L/\partial \lambda &= A_S{}' e^z - XYZ_S = 0, \end{aligned} \tag{7}$$

and solving for z and λ yields a stationary point, which for this particular equality-constrained quadratic program is a minimum and a solution. This $(n + 3) \times (n + 3)$ system of nonlinear equations is readily solved by Newton's method. Defining the vector-valued function, F, as

$$F = \begin{Bmatrix} Cz + \mathrm{diag}(e^z)A_S\lambda \\ A_S{}'e^z - XYZ_S \end{Bmatrix}, \tag{8}$$

and the Jacobian matrix of first partial derivatives of F as

$$J = \left[\begin{array}{c|c} C + \mathrm{diag}(\mathrm{diag}(e^z)A_S\lambda) & \mathrm{diag}(e^z)\ A_S \\ \hline A_S{}'\mathrm{diag}(e^z) & 0 \end{array}\right], \tag{9}$$

the change in the values of z and λ with each Newton iteration is found by solving the linear system

$$J \begin{Bmatrix} \Delta z \\ \Delta\lambda \end{Bmatrix} = -F. \tag{10}$$

Thus, a reconstructed reflectance curve can be found with a series of linear equation solutions, updating z and λ each iteration: $z^{k+1} = z^k + \Delta z$ and $\lambda^{k+1} = \lambda^k + \Delta\lambda$. Convergence is rapid and tests on 140 000 cases show that a solution to within a tolerance of $|F| < 10^{-8}$ is obtained with a mean number of iterations of 6.8.

As an interesting side note, due to the nature of this equality-constrained quadratic program, there is a unique reflectance curve with minimum-slope-squared properties for a given tristimulus value triplet. In other words, there is a one-to-one correspondence between these optimal reflectance curves and their corresponding tristimulus values. Either can be used interchangeably as a canonical representation of a specific color.

Below is a MATLAB function that performs the spectral reconstruction. This code also works in the free and open-source Octave software.[44] It accepts as input arguments the source-referenced CMFs, *As*, the matrix of finite-differencing constants, *C*, and the source tristimulus values, *XYZ*, and returns the spectral reconstruction, ρ.

```
function rho=spectral_recon(As, C, XYZ)
% As is nx3 Ws-referenced CMFs, As = diag(Ws)*A
% C is nxn matrix of finite-differencing constants
  (Eqn 5)
% XYZ is a 3x1 vector of target Ws-referenced
  tristimulus values
% rho is a nx1 vector of reflectance values (or zeros if
  failure)
n=size(As,1);
rho = zeros(n,1);
z=zeros(n,1);
lambda=zeros(3,1);
count=0;
maxit=20; % max number of iterations
ftol=1.0e-8; % solution tolerance
while count <= maxit
  r=exp(z);
  dr=diag(r);
  v=dr*As*lambda;
```

```
  F=[C*z+v; As'*r-XYZ];
  J=[C+diag(v), dr*As; As'*dr, zeros(3)];
  delta=J\(-F); % solve system of equations J*delta = -F
  z=z+delta(1:n);
  lambda=lambda+delta(n+1:n+3);
  if all(abs(F)<ftol)
    rho=exp(z);
    return
  end
  count=count+1;
end
```

Since this code will be executed once for each corresponding color prediction, it is best to precompute *As* and *C* and pass them as input arguments. The function will fail if improper inputs are provided, such as *XYZ* outside the spectral locus. The online supplementary documentation provides a worked example of this reconstruction.[45]

6 | IMPLEMENTING THE CAT

This section outlines how the spectral reconstruction method can be implemented as a CAT, with MATLAB/Octave code snippets included for clarity. It is assumed that the three inputs are the source and destination illuminant white points, XYZ_S^{wp} and XYZ_D^{wp}, and the source-illuminant-referenced color, XYZ_S.

1. If the illuminant white points provided are scaled so that $Y = 100$, divide them by 100 to conform with the tristimulus value scaling convention (0-1) used throughout this presentation. Similarly, scale XYZ_S to the 0 to 1 convention if provided in the 0 to 100 range.
2. Generate the source and destination illuminant vectors, W_S and W_D, from XYZ_S^{wp} and XYZ_D^{wp} using the spectral reconstruction code above, replacing input parameter A_S with the unweighted CMFs A:

```
Ws=spectral_recon(A, C, XYZwps);
Wd=spectral_recon(A, C, XYZwpd);
```

This will produce illuminants that are properly normalized (scalar product $\overline{y}' \cdot W = 1$).

3. Compute illuminant-referenced CMFs $A_S = \overline{W_S}\, A$ and $A_D = \overline{W_D}\, A$ (overbar indicates a diagonal matrix created from the specified vector).

```
As=diag(Ws)*A;
Ad=diag(Wd)*A;
```

4. Create the finite-differencing coefficients matrix, C, as shown in Equation (5). One way to do this is with the MATLAB/octave statements

```
C=full(gallery('tridiag',n,-2,4,-2));
C(1,1)=2;
C(n,n)=2;
```

where n is the number of rows of matrix A.

The above steps need to be performed only once for a given source/destination illuminant pair. The remaining steps (5-7) are done for each corresponding color destination prediction.

5. Generate a reflectance reconstruction from the source color, XYZ_S:

```
rho=spectral_recon(As, C, XYZs);
```

6. Compute the unadjusted destination color, $XYZ_D = A_D{}' \rho$:

```
XYZd=Ad'*rho;
```

7. Adjust XYZ_D so that it preserves its chromaticity coordinates, (x, y), while having a Y value that matches the Y value of XYZ_S. Call this XYZ_{Dp}, which is the predicted W_D-referenced destination color forming a corresponding color pair with XYZ_S.

```
XYZdp=XYZd*XYZs(2)/XYZd(2);
```

7 | SYMMETRY

In some applications, it is desirable that the CAT be symmetric, that is, if a source color is transformed from illuminant 1 to illuminant 2, and then the destination color obtained is transformed from illuminant 2 back to illuminant 1, the resulting destination color should match the original source color. With the CAT proposed above, there may be a small mismatch.

TABLE 3 Code changes to make the proposed method symmetric

Line	Original code	Symmetric code
1	`function rho=spectral_recon(As,C,XYZ)`	`function rho=spectral_recon_sym(As,Asd,C, XYZ)`
16	`v=dr*As*lambda;`	`v=dr*Asd*lambda;`
18	`J=[C+diag(v),dr*As; As'*dr,zeros(3)];`	`J=[C+diag(v),dr*Asd; As'*dr,zeros(3)];`

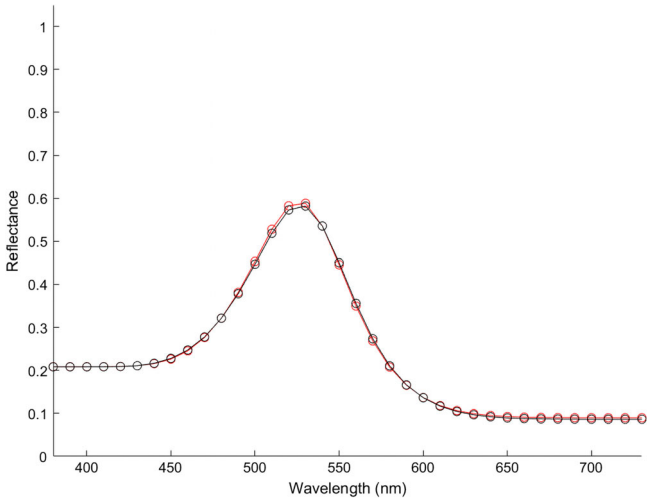

FIGURE 4 Reconstructed reflectance curve for original proposed method (black) and symmetric version (red)

This can easily be corrected, however, by a slight modification to the proposed method. We define a "dual-referenced" CMF as

$$A_{SD} = \overline{W_S}\ \overline{W_D}\ A = \overline{W_D}\ A_S \tag{11}$$

This dual referenced CMF replaces some instances of A_S in the system of nonlinear equations

$$F = \begin{Bmatrix} Cz + \mathrm{diag}(e^z) A_{SD} \lambda \\ A_S{}' e^z - XYZ_S \end{Bmatrix} \tag{11}$$

and in the corresponding Jacobian matrix

$$J = \left[\begin{array}{c|c} C + \mathrm{diag}(\mathrm{diag}(e^z) A_{SD} \lambda) & \mathrm{diag}(e^z)\ A_{SD} \\ \hline A_S{}' \mathrm{diag}(e^z) & 0 \end{array}\right]. \tag{13}$$

Note that A_{SD} is not used in the second set of equations, as these equations must use A_S to ensure that the reflectance curve has the proper tristimulus values, referenced only to the source illuminant. Justification of this alteration is lengthy and is available in the online supplementary documentation.[46]

Changing the MATLAB/Octave code presented earlier for this symmetric case is a simple matter of modifying three lines, as shown in Table 3.

The change to the reflectance curve is typically quite small. For example, using illuminant A as the source and illuminant D65 as the destination, the source color XYZ_S = (0.2, 0.3, 0.1) produces the two reflectance curves shown in Figure 4 using the original spectral reconstruction and the symmetric version.

The two reflectance curves are virtually identical. However, that small change is sufficient to ensure symmetry, as demonstrated in Table 4.

The symmetric version also performs virtually the same as the original proposed method when applied to the corresponding-colors data sets. Table 5 presents color difference values for both methods and the overall means match to two decimal places.

8 | ROBUSTNESS

The spectral reconstruction used in the proposed method creates reflectance curves that are strictly positive. As a direct consequence, it is impossible for the proposed CAT to generate a destination color outside the spectral locus. The proposed CAT produces destination colors within the spectral locus regardless of the choice of source color and source/destination white points (so long as all three fall within the spectral locus). This performance characteristic is termed "robustness" of the CAT.

To demonstrate this robustness, the proposed CAT (specifically, the symmetric version) is applied to the optimum colors enclosing a Y = 0.3 slice of the object color solid. Equal energy is used as the source illuminant and a series of destination illuminants with white points located 90% from equal energy to the spectral locus are selected at nine equally spaced angles from equal energy. Figure 5 demonstrates that in all cases, the destination colors remain inside the spectral locus.

Compare this to the behavior of CAT16 applied to the same conditions, shown in Figure 6. In all nine cases, there is a portion of the object color solid that is projected outside the spectral locus. In some cases, the destination colors produced by CAT16 far exceed the region located outside the spectral locus predicted by Fry to enclose all supersaturated colors (Figure 1 of Reference 16).

Although the proposed CAT performs well to keep destination colors within the spectral locus, it suffers from two main deficiencies in comparison to existing CATs: increased complexity of implementation and increased computational effort. The spectral reconstruction requires

TABLE 4 Comparison of original and symmetric versions

Version	XYZ_A	CAT A to D65 XYZ_{D65}	CAT D65 to A XYZ_A
Original	(0.2, 0.3, 0.1)	(0.1707, 0.3000, 0.2426)	(0.2059, 0.3000, 0.1016)
Symmetric	(0.2, 0.3, 0.1)	(0.1699, 0.3000, 0.2415)	(0.2000, 0.3000, 0.1000)

Note: The fourth column is the outcome of the reversed CAT (D65 to A) applied to the XYZ_{D65} values of the third column.
Abbreviation: CAT, chromatic adaptation transform.

TABLE 5 Comparison of mean ΔE^*_{94} color difference for the original proposed method and the symmetric version

Data set	Original method	Symmetric version
CSAJ	3.72	3.70
Helson	4.10	4.09
Lam & Rigg	3.22	3.22
LUTCHI	4.01	4.03
Kuo & Luo	2.85	2.84
Breneman	5.48	5.47
Braun & Fairchild	4.07	4.08
McCann	9.78	9.78
Mean (all data sets)	**4.74**	**4.74**
Mean (no McCann)	**4.01**	**4.01**

solving a series of simultaneous linear equations, whereas existing CATs require only simple matrix multiplication. Fortunately, implementing the proposed method does not require writing original software for solving the linear systems. The field of numerical linear algebra is mature and public domain software utilities are readily available for solving such systems.[47] These utilities have been available for decades and have been refined over the years to be efficient and robust. They are reliable building blocks for numerical applications such as this.

The other obstacle is computational effort. Linear equation solving requires considerably more computation than simple matrix multiplication, which is all that current CATs require. Based on timed trials of 140 000 cases comparing the execution times of the spectral reconstruction to simple matrix multiplication, the author estimates that a two to three order of magnitude increase in computational effort is required (for the case of $n = 36$). This is a substantial increase, but if robustness of the CAT is of paramount importance, this increase may be justifiable.

9 | DEGREE OF ADAPTATION

Existing CATs implement a parameter, D, to address partial adaptation. It is set between 1 and 0 according to the viewing conditions. The diagonal matrix of von Kries coefficients, Λ, comprising ratios of destination to source

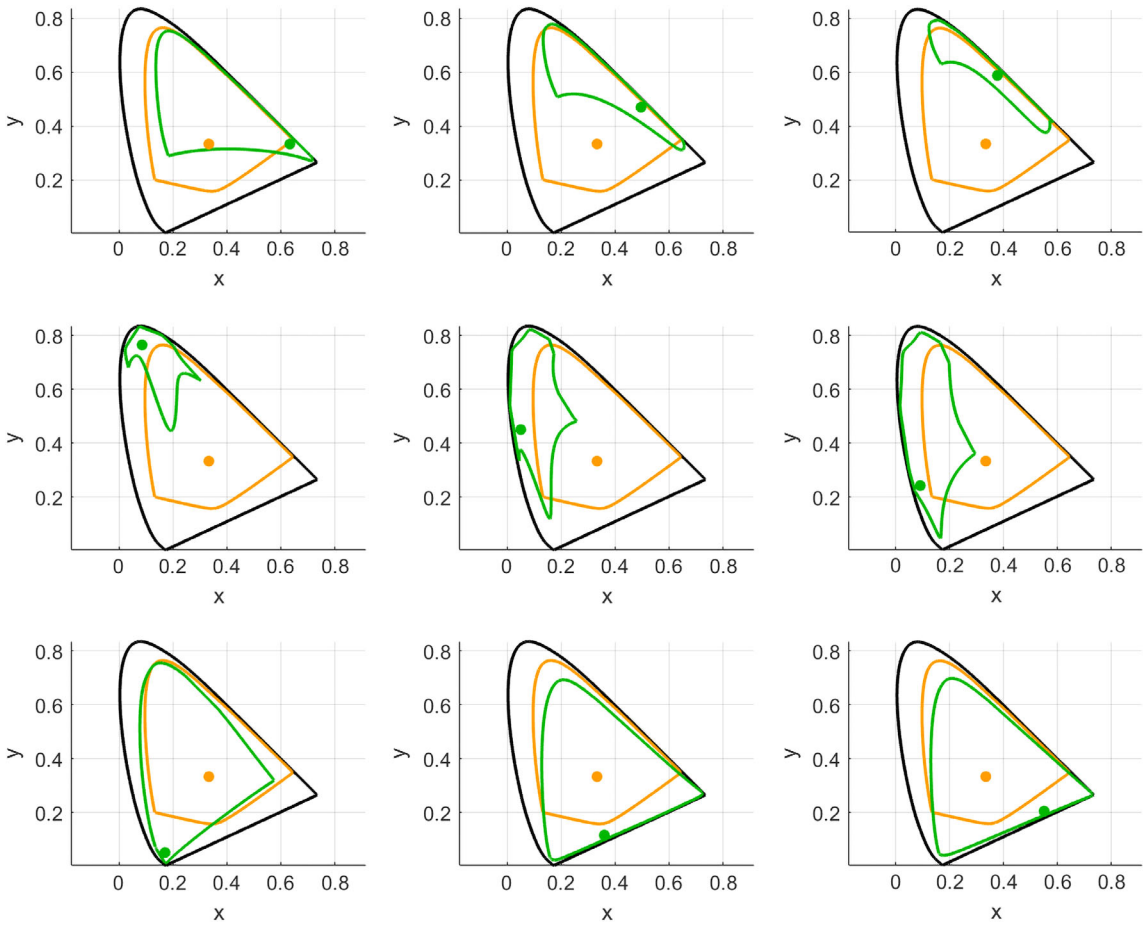

FIGURE 5 The proposed CAT applied to a $Y = 0.3$ slice of the object color solid, using equal energy as the source illuminant (orange) and a variety of destination illuminants that are 90% toward the spectral locus (green). CAT, chromatic adaptation transform

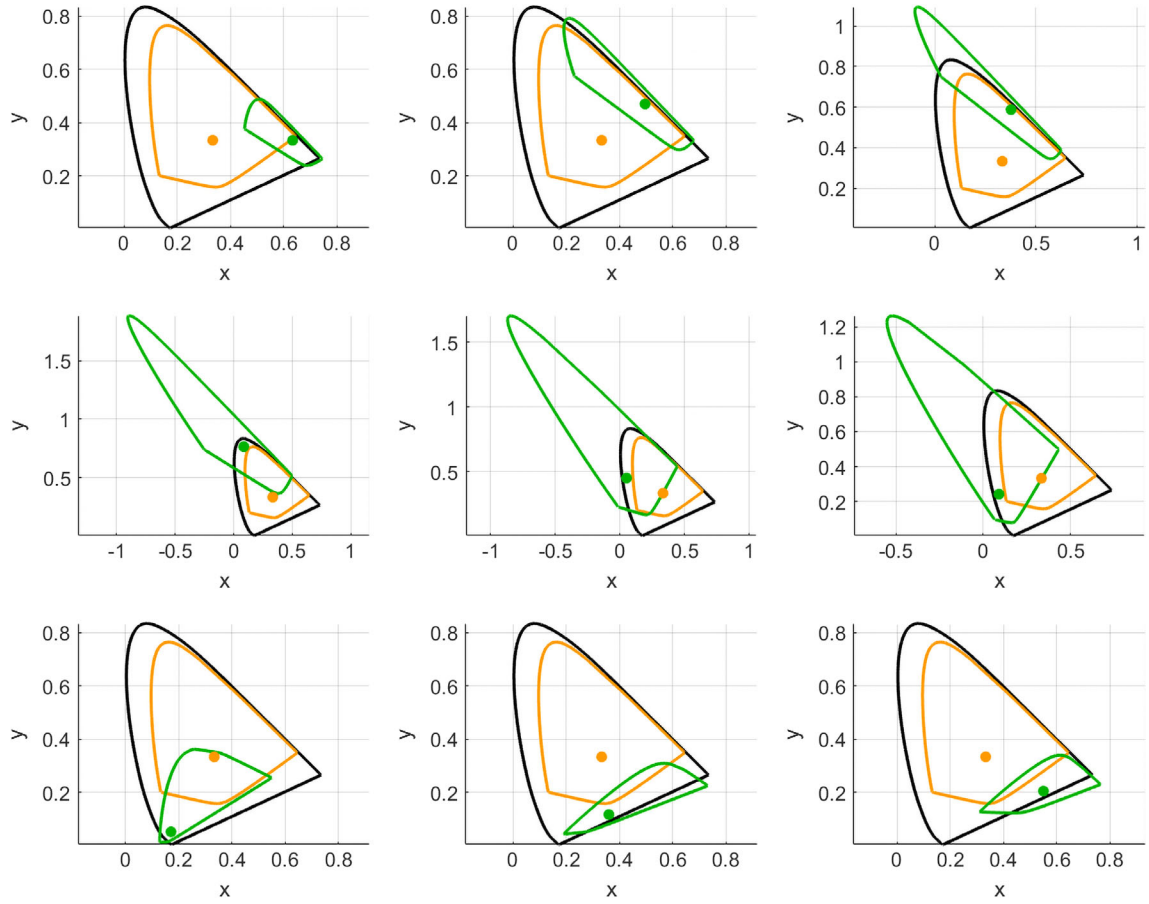

FIGURE 6 CAT16 applied to the same conditions of Figure 5

illuminant white points, is parametrically shifted toward the identity matrix as D approaches zero:

$$\Lambda_{adapt} = D\ \Lambda + (1-D)\ I. \tag{14}$$

A similar linear parametric treatment could be applied to the proposed method by adjusting the destination illuminant toward the source illuminant using D:

$$W_{D,adapt} = D\ W_D + (1-D)\ W_S. \tag{15}$$

As D approaches zero, the source and destination illuminants become the same and the destination color equals the source color, just as with the $D = 0$ case in existing CATs.

The author has not investigated how this partial adaptation treatment compares to the standard treatment. It is a suggested topic for future investigation.

10 | CONCLUSIONS

A proposed CAT has been presented that is based on a spectral reconstruction algorithm, specifically, one that computes the unique spectral distribution within a metameric suite that has minimum slope squared in log space. The reflectance curves thus generated tend to show good similarity to reflectance curves of many object colors found in nature, specifically, commercial paints and natural pigments. The proposed CAT simply computes the effect that changing the illuminant has on tristimulus values computed from the reflectances, using standard CMF calculations. While this approach appears to ignore the phenomenon of adaptation, focusing instead on techniques more closely related to color constancy, the corresponding-color pairs it generates match the empirical corresponding-colors data sets as well as or better than existing CATs. The proposed CAT does not use the empirical corresponding-colors data sets to "tune" performance like the most recent CATs do. It should be noted that although the proposed method uses a spectral reconstruction as an intermediate stage of the process, its inputs are the same as those for traditional CATs, namely, tristimulus values of source colors and illuminant white points.

The proposed CAT is completely immune to producing destination colors located outside the spectral locus or having negative tristimulus values. This performance feature comes with an increase in complexity and a significant increase in computational effort. If avoidance of destination colors outside the spectral locus or having negative tristimulus values is of primary importance, then this increase may be justifiable.

ORCID

Scott A. Burns https://orcid.org/0000-0002-1251-7758

REFERENCES

[1] Fairchild MD. *Color Appearance Models*. 3rd ed. Chichester, UK: Wiley; 2013.

[2] Luo MR, Li CJ. Chapter 11: CIE color appearance models and associated color spaces. In: Schanda J, ed. *Colorimetry: Understanding the CIE System*. Hoboken, NJ: Wiley; 2007:255-290.

[3] Hunt RWG, Li C, Luo MR. Chromatic adaptation transforms. *Color Res Appl*. 2005;30(1):69-71.

[4] Kries V. *Chromatic Adaptation* Festschrift der Albrecht-Ludwig-Universitat (Fribourg); 1902. [Translation: MacAdam DL. Sources of Color Science]. Cambridge, MA: MIT Press; 1970.

[5] Luo MR, Rhodes PA. Corresponding-colour data sets. *Color Res Appl*. 1999;24(4):295-296.

[6] Table II: The Data File Names and Number of Samples in Each Experimental Data Set. https://bit.ly/2v7mJA7. (Expands to https://web.archive.org/web/20040225194527/http://colour.derby.ac.uk/colour/info/catweb/table2.html). Accessed April 16, 2019.

[7] Brill MH. Irregularity in CIECAM02 and its avoidance. *Color Res Appl*. 2006;31(2):142-145.

[8] Brill MH, Susstrunk S. Repairing gamut problems in CIECAM02: a progress report. *Color Res Appl*. 2008;33(5):424-426.

[9] Li C, Perales E, Luo MR, Martinez-Verdu F. Mathematical approach for predicting non-negative tristimulus values using the CAT02 chromatic adaptation transform. *Color Res Appl*. 2012;37(4):255-260.

[10] Brill MH, Mahy M. Visualization of mathematical inconsistencies in CIECAM02. *Color Res Appl*. 2013;38(3):188-195.

[11] Li C, Ji C, Luo R, Melgosa M, Brill MH. CAT02 and HPE triangles. *Color Res Appl*. 2015;40(1):30-39.

[12] Li C, Li Z, Wang Z, et al. A revision of CIECAM02 and its CAT and UCS. In Proceedings of the 24th Color and Imaging Conference, Society for Imaging Science and Technology, San Diego, California; November 7-11, 2016:208-212.

[13] Li C, Li Z, Wang Z, et al. Comprehensive color solutions: CAM16, CAT16, and CAM16-UCS. *Color Res Appl*. 2017;42:703-718.

[14] CIE Publ. 160. A Review of Chromatic Adaptation Transforms. Vienna, Austria: CIE Central Bureau; 2004.

[15] CIE Publ. 159. A Colour Appearance Model for Colour Management Systems: CIECAM02. Vienna, Austria: CIE Central Bureau; 2004.

[16] Fry G. Colors of maximal saturation. *Optom Vis Sci*. 1995;72(8):541-546.

[17] Hunt RWG. Revised colour-appearance model for related and unrelated colours. *Color Res Appl*. 1991;16(3):146-165.

[18] Estévez O. On the Fundamental Data-Base of Normal and Dichromatic Color Vision [PhD thesis]. Amsterdam, The Netherlands: University of Amsterdam, Krips Repro Meppel; 1979.

[19] Wyszecki G, Stiles WS. *Color Science, Concepts and Methods, Quantitative Data and Formulae*. 2nd ed. New York, NY: John Wiley & Sons; 1982:179-183.

[20] Supplementary Documentation. 2. Examples of CATs Producing Negative Tristimulus Values. http://scottburns.us/supplementary-documentation/#Sec2. Accessed April 16, 2019.

[21] Supplementary Documentation. 4. Chromatic Adaptation Transform by Spectral Reconstruction. http://scottburns.us/supplementary-documentation/#Sec4. Accessed April 16, 2019.

[22] Burns SA. Generating Reflectance Curves from sRGB Triplets. http://scottburns.us/reflectance-curves-from-srgb/. Accessed April 16, 2019.

[23] Trigt CV. Smoothest reflectance functions. I. Definition and main results. *J Opt Soc Am A*. 1990;7(10):1891-1904.

[24] Trigt CV. Smoothest reflectance functions. II. Complete results. *J Opt Soc Am A*. 1990;7(12):2208-2222.

[25] Hawkyard CJ. Synthetic reflectance curves by subtractive colour mixing. *J Soc Dyers Colourists*. 1993;109:246-251.

[26] Hawkyard CJ. Synthetic reflectance curves by additive mixing. *J Soc Dyers Colourists*. 1993;109:323-329.

[27] Smits B. An RGB-to-spectrum conversion for reflectances. *J Graph Tools*. 1999;4(4):11-22.

[28] Dupont D. Study of the reconstruction of reflectance curves based on tristimulus values: comparison of methods of optimization. *Color Res Appl*. 2002;27(2):88-99.

[29] Wang G, Li C, Luo MR. Improving the Hawkyard method for generating reflectance functions. *Color Res Appl*. 2005;30(4):283-287.

[30] Attarchi N, Amirshahi SH. Reconstruction of reflectance data by modification of Berns' Gaussian method. *Color Res Appl*. 2009;34(1):26-32.

[31] Abed FM, Amirshahi SH, Abed MRM. Reconstruction of reflectance data using an interpolation technique. *J Opt Soc Am A Opt Image Sci Vis*. 2009;26(3):613-624.

[32] Bianco S. Reflectance spectra recovery from tristimulus values by adaptive estimation with metameric shape correction. *J Opt Soc Am A Opt Image Sci Vis*. 2010;27(8):1868-1877.

[33] Amirshahi SH, Amerhahi SA. Adaptive non-negative bases for reconstruction of spectral data from colorimetric information. *Opt Rev*. 2010;17(6):562-569.

[34] Babaei V, Amirshahi SH, Agahian F. Using weighted pseudo-inverse method for reconstruction of reflectance spectra and analyzing the dataset in terms of normality. *Color Res Appl*. 2011;36(4):295-305.

[35] Kim BG, Han J, Park S. Spectral reflectivity recovery from the tristimulus values using a hybrid method. *J Opt Soc Am A*. 2012;29(12):2612-2621.

[36] Kim BG, Werner JS, Siminovitch M, Papamichael K, Han J, Park S. Spectral reflectivity recovery from tristimulus values using 3D extrapolation with 3D interpolation. *J Opt Soc Korea*. 2014;18(5):507-516.

[37] Amiri MM, Amirshahi SH. A hybrid of weighted regression and linear models for extraction of reflectance spectra from CIEXYZ tristimulus values. *Opt Rev*. 2014;21(6):816-825.

[38] Amiri MM, Amirshahi SH. A step by step recovery of spectral data from colorimetric information. *J Opt*. 2015;44(4):373-383.

[39] Inoue K, Hara K, Urahama K. Reflectance spectra recovery with non-negativity constraints. In: 2016 International Symposium on Intelligent Signal Processing and Communication Systems (ISPACS), Phuket; 2016:1-6.

[40] Cao B, Liao N, Li Y, Cheng H. Improving reflectance reconstruction from tristimulus values by adaptively combining colorimetric and reflectance similarities. *Opt Eng*. 2017;56(5):053104.

[41] Otsu H, Yamamoto M, Hachisuka T. Reproducing spectral reflectances from tristimulus colours. *Comput Graph Forum*. 2018;37(6):370-381.

[42] Fairchild MD. Spectral adaptation. *Color Res Appl*. 2007;32:100-112.

[43] Fairchild MD. Spectral adaptation: a reason to use the wavenumber scale. In: IS&T/SID 14th Color Imaging Conference, Scottsdale; November 6-10, 2006:314-319.
[44] GNU Octave Scientific Programming Language. https://www.gnu.org/software/octave/. Accessed April 16, 2019.
[45] Supplementary Documentation. 5. Spectral Reconstruction Computation. http://scottburns.us/supplementary-documentation/#Sec5. Accessed April 16, 2019.
[46] Supplementary Documentation. 7. Symmetry. http://scottburns.us/supplementary-documentation/#Sec7. Accessed April 16, 2019.
[47] Wikipedia search of "Comparison of Linear Algebra Libraries". https://bit.ly/2IGkDPX. Accessed April 16, 2019.

AUTHOR BIOGRAPHY

Scott A. Burns is a retired engineering professor at the University of Illinois at Urbana-Champaign (UIUC). He has been interested in colorimetry since the 1980s, when he was introduced to the topic by his colleague Jozef Cohen. His other research interests include engineering design methodology, structural design, mechanism design, mechatronics, and data visualization. He received a National Science Foundation Presidential Young Investigator award in 1989 and a UIUC College of Engineering Everitt Award for Teaching Excellence in 1990, and he was named a fellow in the UIUC Center for Advanced Study in 1992, and received two State-of-the-Art in Civil Engineering awards from ASCE in 1998 and 2004.

How to cite this article: Burns SA. Chromatic adaptation transform by spectral reconstruction. *Color Res Appl*. 2019;44:682–693. https://doi.org/10.1002/col.22384